Vibrational Spectroscopy 90 (2017) 81–88

Contents lists available at ScienceDirect

Vibrational Spectroscopy

journal homepage: www.elsevier.com/locate/vibspec

The improvements on TiO_2 catalyzed AgNPs based SERS substrate and detection methods

Huaizhou Jin[a,b], Qipeng Lu[a,*], Shangzhong Jin[c], Haiquan Ding[a], Hongzhi Gao[a], Xingdan Chen[a], Yanqiu Zou[c]

[a] State Key Laboratory of Applied Optics, Changchun Institute of Optics, Fine Mechanics and Physics, Chinese Academy of Sciences, Changchun, Jilin, China
[b] University of Chinese Academy of Sciences, Beijing, China
[c] Key Laboratory of Zhejiang Province on Modern Measurement Technology and Instruments, Jiliang University, Hangzhou, China

ARTICLE INFO

Article history:
Received 22 November 2016
Accepted 17 March 2017
Available online 13 April 2017

Keywords:
Surface enhanced Raman spectroscopy
Silver nano-particles
Photo-catalysis
Titanium dioxide

ABSTRACT

Using TiO_2 on slides to facilitate photo-catalysis of silver nano-particles (AgNPs) is a simple and versatile way of making silver based solid SERS substrates. However, due to the difficulty of getting optimal surface AgNPs structure, it is difficult to reach optimal enhancement factor or measurement uniformity with this method. In this research, production conditions and setups, ranging from dip-coating to photo-catalysis are investigated. Spectral analysis show that some conditions, such as time of calcination and the purity of UV light used in photo-catalysis, affect the resulting SERS substrates more significantly. The overall performance of substrates made using this method is increased; sensitivity is increased so that the limit of detection for Rhodamin 6G (R6G) is as low as 10^{-8} M, and the signature peak of R6G at 1650 cm^{-1} measured from different spots on substrates has a standard deviation of less than 20%.

1. Introduction

Raman spectroscopy is a well-established analytical technique based on the inelastic scattering of monochromatic light by the vibrating atoms constituting the sample. It is widely used in fields such as materials, food, medicine, chemistry and so on [1–5].

One of Raman spectroscopy's main disadvantages is its relatively weak signal strength. The discovery of Surface enhanced Raman scattering (SERS) can be used to overcome this disadvantage. SERS was discovered by Fleischmann et al. in 1974 and later confirmed by Van Duyne et al. in 1977 [6–8]. SERS enhancement factor ranges from 10^8 to 10^{14}, so trace amounts of molecules become detectable [4,8–10].

For SERS to take effect, the sample molecules must be adsorbed on to the surface of metal nano-particles, most notably silver (AgNPs) or gold nano-particles (AuNPs) [3,4,11]. Multiple metal nano-particles aggregated together can increase the SERS enhancement factors [3,4,11,12], which is essential for the detection of trace substances. Ordered nano-structures can further enhance Raman signals because of possible long-range ordering coupling effect [13].

There are usually two types of SERS substrates: a) nano-particle colloidal made from Lee and Miesal or similar methods [14] and b) solid substrates that come from various methods, such as deposition of nano-particle colloidal, reduction of silver nitrate ($AgNO_3$) or chloroauric acid ($HAuCl_4$), or nano-rod array structures made through self-assembly, deposition methods or Lithographic and Template Synthesis [15–21]. This study focuses on solid substrates, which show advantages when used to enhance certain types of samples, such as samples that contain large protein molecules [3,5].

One method of making AgNPs based solid substrates is using TiO_2 as a catalyst to facilitate the reduction of $AgNO_3$ under UV light [12,22,23], and then have the AgNPs adsorb on to TiO_2 [24,25]. This method takes relatively short time, is inexpensive and can be used to produce multiple substrates at once. As a chemical self-assembly method, its control over the surface structure and morphology of AgNPs is limited, when compared to methods such as glancing angle deposition (GLAD) physical vapor deposition [26], Lithographic and Template Synthesis [20,21], and it can be difficult to achieve optimal enhancement factor and uniformity.

* Corresponding author at: State Key Laboratory of Applied Optics, Changchun Institute of Optics, Fine Mechanics and Physics, Chinese Academy of Sciences, Changchun, Jilin, China.
E-mail addresses: 18367198456@163.com (H. Jin), luqipeng@126.com (Q. Lu).

http://dx.doi.org/10.1016/j.vibspec.2017.03.005
0924-2031/

2. Materials and production of TiO_2 photo-catalyzed AgNPs substrates

Analytically pure Tetrabutyl titanate, acetylacetonate, nitric silver ($AgNO_3$), Rhodamin 6G (R6G), nitric acid, ethanol, as well as glass and quartz slides are purchased from Hangzhou Mike Chemical Instruments Co., Ltd.

Method for making TiO_2 photo-catalyzed AgNPs substrates are derived and improved on the basis of methods by Li et al. and Mazzocut et al. [12,22]. The steps of the production process are as follows:

2.1. Making TiO_2 sol-gel

The first step is to make TiO_2 sol-gel. Two solutions, solution A and solution B are prepared. Solution A is made by mixing 50 mL of Tetrabutyl titanate with 3 mL of acetylacetonate. Magnetically stir solution A for 10 min. Solution B is made by mixing 110 mL of 95% ethanol, 1.4 mL deionized water and 0.2 mL nitric acid. Solution B is also magnetically stirred for 10 min after mixing the three reagents.

After solutions A and B are made, solution B is added into solution A drop by drop, under magnetic stir. After all of solution B is added into solution A, continue magnetic stirring for 30 min.

2.2. Deposition of TiO_2

Before coating, the glass or quartz slides are washed using ethanol and then deionized water and then oven dried at 50 °C.

Then, coat TiO_2 on the slides using dip coating techniques. Different dipping speed would affect the thickness of TiO_2. Dipping speeds ranging from 100 mm/min to 300 mm/min have been tested. The slide stays in the solution for 2 min during dip coating. Then, the slide rests on a flat surface for 30 min before calcination.

2.3. Calcination

The goal of the calcination step is to turn the amorphous TiO_2 sol-gel on the slides into anatase form, which will act as the catalyst as the photo-catalysis step, as well as the spots for AgNPs to adsorb on to. Thus, the surface structure of TiO_2 on the slides will become an important factor in determining the surface structure of AgNPs, which determines the enhancement factor, as well as uniformity.

Around 400 °C, TiO_2 starts transforming into anatase form; however, around 550 to 600 °C, part of TiO_2 would begin transforming into rutile form, which is not as effective as catalyst or adsorbent for the deposition of AgNPs [12,27]. Therefore, temperature needs to be kept within the range between 450 and 550 °C.

The coated glass or quartz slide is calcined in a muffle furnace. After the slides are inside the furnace, the furnace is heated to around 500 °C in 30 min and stays at that temperature for 60 min. Different temperatures from 450° to 550° (at this range of temperature, amorphous TiO_2 began morphing into anatase form) are used and compared. After heating for 60 min, the heat is turned off and the furnace cools down naturally.

After the temperature in furnace drops to 300°, open the furnace hatch to let it cool down faster. Then, remove the calcined slides from the muffle furnace.

2.4. Photo-catalysis

The $AgNO_3$ solution is made by mixing 0.2548 g of $AgNO_3$ powder with 500 mL deionized water. Magnetically stir for 10 min.

The slides, after calcination, are cut into 5×5 mm pieces and put inside a culture dish. Pour $AgNO_3$ solution slowly into the dish, and make sure all slides are immersed in the solution instead of floating on the surface. Different immersion depths from 3 mm to 10 mm (meaning the how much the $AgNO_3$ solution level is higher than the top surface of the slides) are used and compared.

A 24W UV lamp is used for the photo-catalysis of the substrates. Two different wavelengths of UV light are used for photo-catalysis: 254 nm and 365 nm. A filter is also used to block most of the visible light emitted from the UV lamp during photo-catalysis for comparison. The time of photo-catalysis ranges from 30 min to 90 min for comparison.

After photo-catalysis, the resulting substrates are washed with deionized water and then oven dry at 50 °C for 10 min.

2.5. Gold deposition

Normally, silver based SERS enhancement substrates are unstable and are vulnerable to oxidation when exposed in air. Coating a protective film is a common way to separate silver from air; for example, methods that coat Al_2O_3 or SiO_2 on silver substrates are developed [28]. In this research, a gold deposition method is used on the substrates so that a thin layer (around 3 nm think) of gold are deposited on the substrates, and are compared to substrates without gold deposition.

3. Measurement instrumentation and methods

3.1. TiO_2 and AgNPs morphology measurement

Before photo-catalysis, the thickness and refractive index of TiO_2 on glass would be measured using a Horiba Jobin-Yvon Uvisel ellipsometer, both before and after calcination. Then, TeScan Vega3 scanning electron microscope (SEM) was used to observe the morphology of AgNPs on the substrates.

3.2. SERS measurement

Raman measurement was carried out using Horiba LabRAM Evolution, with a 50 mW 532 nm laser module. R6G (1.0×10^{-5}M to 1.0×10^{-7}M) is used to test the effectiveness of our SERS substrates. First, a small piece (5×5 mm) of substrate is immersed into the Rhodamin 6G solution for 30 min, and then the substrate is oven dried (50 °C) for 10 min before testing. 5% laser power is used for measurement to avoid damaging the substrate or the samples and measure for 5 s as a standard measurement. The average of standard measurements on 10 different spots on 5 substrates made using the same production setup (a total of 50 measurements) is used to compare the performance between different production setups.

Table 1
Thickness as a factor of dip speed on glass slide, measured by ellipsometry.

Dip speed(mm/min)	170	180	190	200	210	220	230
Thickness (nm, BC)	564.1	643.6	758.9	696.3	723.2	770.1	795.9
n(BC)	1.671	1.633	1.630	1.634	1.637	1.631	1.630
χ^2 (BC)	2.41	0.63	0.59	0.55	0.61	0.68	0.58
Thickness (nm, AC)	229.5	295.2	318.2	305.9	294.3	215.1	375.4
n (AC)	2.003	1.924	2.042	2.008	2.107	1.891	2.899
χ^2 (AC)	5.83	10.30	10.28	15.11	13.98	37.00	36.34

Table 2
Thickness as a factor of dip speed on quartz slide, measured by ellipsometry.

Dip speed(mm/min)	170	180	190	200	210	220	230
Thickness (nm, BC)	557.4	636.8	760.1	692.3	731.7	768.8	800.7
n(BC)	1.632	1.630	1.638	1.634	1.664	1.640	1.621
χ^2 (BC)	0.63	0.79	0.56	0.82	1.61	0.55	0.62
Thickness(nm, AC)	139.7	142.0	172.6	180.4	189.7	205.0	233.4
n(AC)	2.151	2.595	2.270	2.260	2.347	2.239	2.171
χ^2 (AC)	4.80	7.29	8.97	3.76	7.62	8.47	5.22

4. Results and analysis

4.1. Ellipsometry results

Ellipsometry results are as follows. For each slide, ten spots on the slide are measured using the ellipsometer, and the average of the values on glass and quartz slides are presented in Tables 1 and 2.

BC and AC stands for before calcination and after calcination, respectively. n refers to the refractive index at wavelength 532 nm χ^2 represents ellipsometry simulation convergence error; according to Horiba Jobin-Yvon, a good simulation would have a χ^2 value of less than 10, and a higher χ^2 value indicates difficulty in finding a good simulation.

Thickness of TiO_2 before calcination is positively correlated to the dipping speed. Also, before calcination, the thickness and n values of TiO_2 dip coated on glass slide are similar to that of TiO_2 dip coated on quartz slide. Higher dipping speed would result in a thicker layer of TiO_2. It seems that the TiO_2 sol-gel layer has refractive index n of around 1.630, which means the dip-coated TiO_2 film includes water, dissolved air and other organic matter. Refractive index result of dip speed at 170 mm/min (glass slide) is 1.671, but that measurement has a higher χ^2 value, indicating that measurement is less accurate.

After calcination, water, dissolved air and organic matter were released into the air during calcination. Thus the dip-coated layers on the slides become much thinner and have higher refractive indices. However, both thickness and n of TiO_2 on the glass slide becomes erratic after calcination. The χ^2 values of these ellipsometry measurements are also much larger with most χ^2 values larger than 10, indicating difficulties of getting an accurate simulation. This is due to glass being heat sensitive; when heated to over 500 °C, the shape and morphology of glass changes and the contact surface becomes irregular, causing difficulties for refractive index measurement and ellipsometry simulations.

On the other hand, thickness values of TiO_2 on the quartz slides are still positively correlated to the dipping speed; the n values do not appear to change much with different dipping speeds. The χ^2 values are still larger than that of before calcination results, but they are still less than 10, within acceptable ranges.

4.2. Comparison between different production setups

4.2.1. Glass vs. quartz slides

The SEM results of AgNPs photo-catalyzed on glass slide vs. that photo-catalyzed on quartz slide are shown in Fig. 1(a) and (b). According to Fig. 1, the substrate photo-catalyzed on quartz slide is more dense, and most of the particles are more regularly (spherical) shaped, while the substrate photo-catalyzed on glass slide has more irregularly shaped nano-particles, and they are more loosely distributed.

In Fig. 1(c) and (d), as well as other spectral figures in this manuscript, 620, 1205, 1358, 1510 and 1650 cm^{-1} are typical Rhodamin 6G Raman peaks. Quartz slides provide more uniform

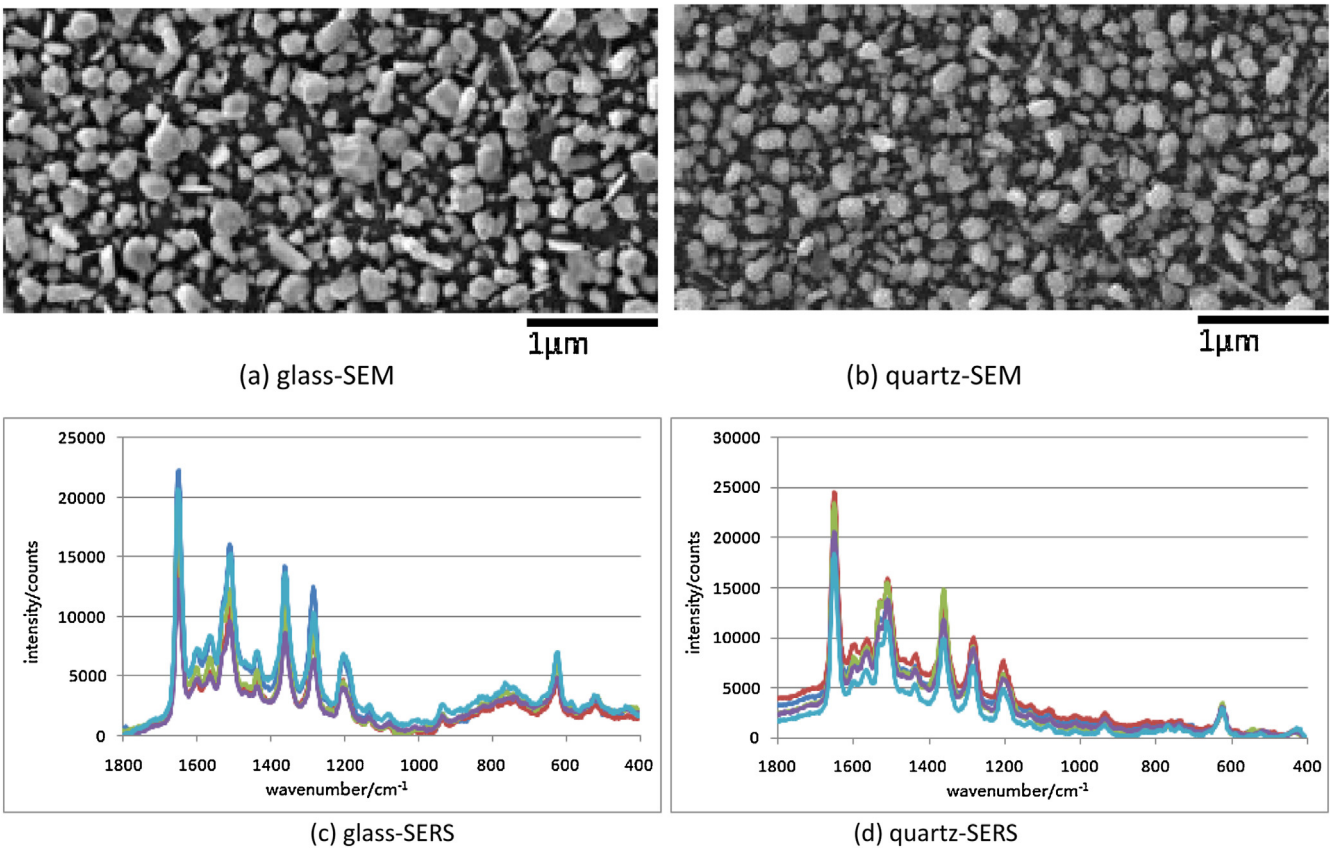

Fig. 1. Comparison between substrates made with glass and quartz slides.

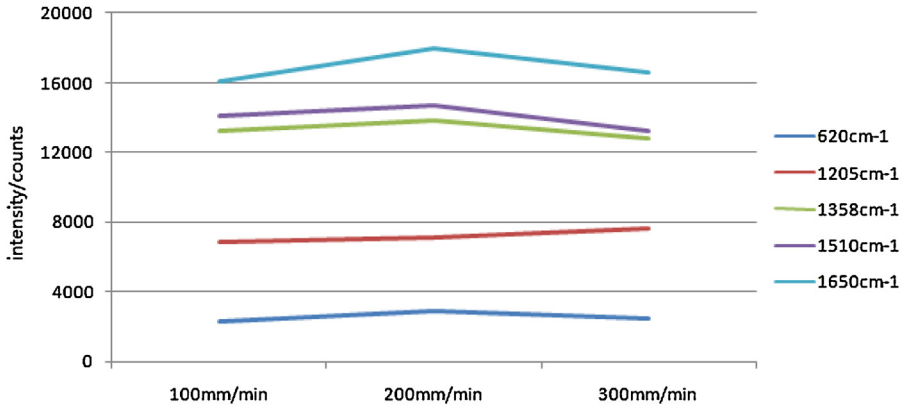

Fig. 2. SERS intensities of the five signature peaks using substrates made with different dip-coating speeds.

and stable Raman results than glass slides; the standard deviation (STD) for the five peaks (from 620 to 1650 cm^{-1}) are 9.5%, 15.5%, 15.0%, 12.0% and 11.3% to their respective average values for quartz slides, and 18.3%, 23.3%, 23.3%, 21.6% and 21.0% to their respective average values for glass slides.

4.2.2. Dip-coating speeds and calcination setups

According to the ellipsometry results shown in the last section, dip-coating speed is positively related to the thickness of the TiO_2 layer on slides, both before and after calcination. Low dip-coating speed would result in thinner TiO_2 layer. On the other hand, calcination temperatures and time affect the formation of anatase form TiO_2. These conditions might affect the performance of the final substrate.

Figs. 2–4 show the resulting SERS intensities using substrates made with different conditions. According to Figs. 2 and 3, the effect of dip-coating speeds (between 100 and 300 mm/min) or calcination temperatures (between 450 and 550 °C) on the final substrate is relatively insignificant. The intensity differences between the three dip-coating speeds, or between the three calcination temperatures, are not very large: differences between the peaks from different dip-coating speeds are within 29.7% (17.5% if the lowest and relatively unstable 620 cm^{-1} peak is excluded), and differences between the peaks from different calcination temperatures are within 28.1%.

Different calcination times, on the other hand, have a more significant effect on the final SERS enhancement effect. As seen from Fig. 5, 60 min is the superior calcination time; the Raman peaks at 1358, 1510 and 1650 cm^{-1} are significantly higher than the substrates calcined for 30 min and 90 min: the 1650 cm^{-1}peak of the 60 min sample is 49.8% higher than the 30 min sample, and 212.3% higher than the 90 min sample; the 1510 cm^{-1} peak of the 60 min sample is 52.8% and 199.4% higher than that of 30 min and 90 min samples, respectively.

4.2.3. Photo-catalysis setups

For the photo-catalysis step, the solution needs to be at least 4 mm higher than the slides. If the immersion depth is insufficient, there is only a loose layer of AgNPs on the substrate, and the enhancement factor is lower. However, extra immersion depth does not seem to further improve the enhancement factor.

Photo-catalysis of AgNPs requires light from UV range. According to research by Mazzocut et al., filtered 365 nm UV photo-catalysis leads to more uniform size distribution of nanoparticles [22]. However, filter the light could improve the uniformity of photo-catalyzed substrates using other photo-catalysis wavelengths as well. Therefore, the SEM images of substrates photo-catalyzed with two UV wavelengths, 254 nm and 365 nm, both filtered and unfiltered, are compared to find the best photo-catalysis setup.

The substrates photo-catalyzed using 365 nm light (both filtered and unfiltered) did not yield good results. The substrates are black, which means that they are covered with Ag_2O and Ag_2S. These two compounds do not have SERS enhancement capabilities.

The SEM results of substrates catalyzed with 254 nm UV light are in Fig. 3.

As shown in the SEM images in Fig. 5(a) and (b), Substrates photo-catalyzed using filtered UV not only has more uniform size

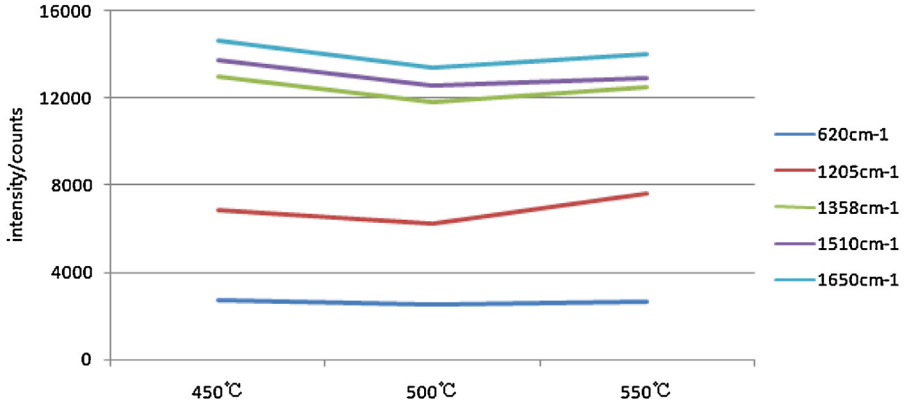

Fig. 3. SERS intensities of the five signature peaks using substrates made with different calcination temperatures.

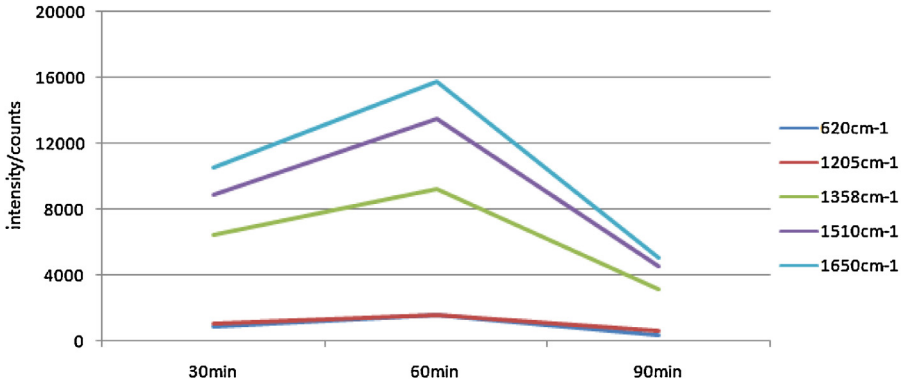

Fig. 4. SERS intensities of the five signature peaks using substrates made with different calcination times from 30 min to 90 min.

distribution of AgNPs, the nano-particles are also smaller and more densely distributed, which is more suitable for SERS enhancement. Raman spectroscopy results, as shown in Fig. 5(c) and (d), are consistent with SEM results; substrates made with filtered 254 nm UV light show more uniform SERS intensities: STD for 620, 1205, 1358, 1510 and 1650 cm^{-1} are 9.9%, 18.6%, 15.0%, 15.0% and 11.3% to their respective average values for the spectra collected from substrates made with filtered UV, and 17.9%, 40.8%, 42.8%, 53.3% and 77.0% to their respective average values for the spectra collected from substrates made with unfiltered UV. Also, from Fig. 5(c), SERS spectra from substrates photo-catalyzed with unfiltered 254 nm UV light show are relatively unstable and show inconsistent peaks, which are not present in Fig. 5(d).

Then, different photo-catalysis times are compared: 60, 90 and 120 min. Results in Fig. 6 show that 90 min is the superior photo-catalysis time and the difference between the three photo-catalysis times are quite significant.

4.3. Gold deposition and substrate longevity

On substrates made using this method, because of the interaction of electron and hole in Anatase, Ag^{+} ions can transform into AgNPs more easily and is thus more resistant to oxidation. However, AgNPs might still be relatively unstable and could become oxidized, which decreases Raman enhancement capabilities. Thus, we deposited a layer of gold, approximately 3 nm think, on to the surface of the AgNPs substrates. The initial SERS comparisons are shown in Fig. 7. The average intensity for the 620 cm^{-1} peak for substrate with gold deposition is 6.6% higher than that of substrate without gold deposition; on the other hand,

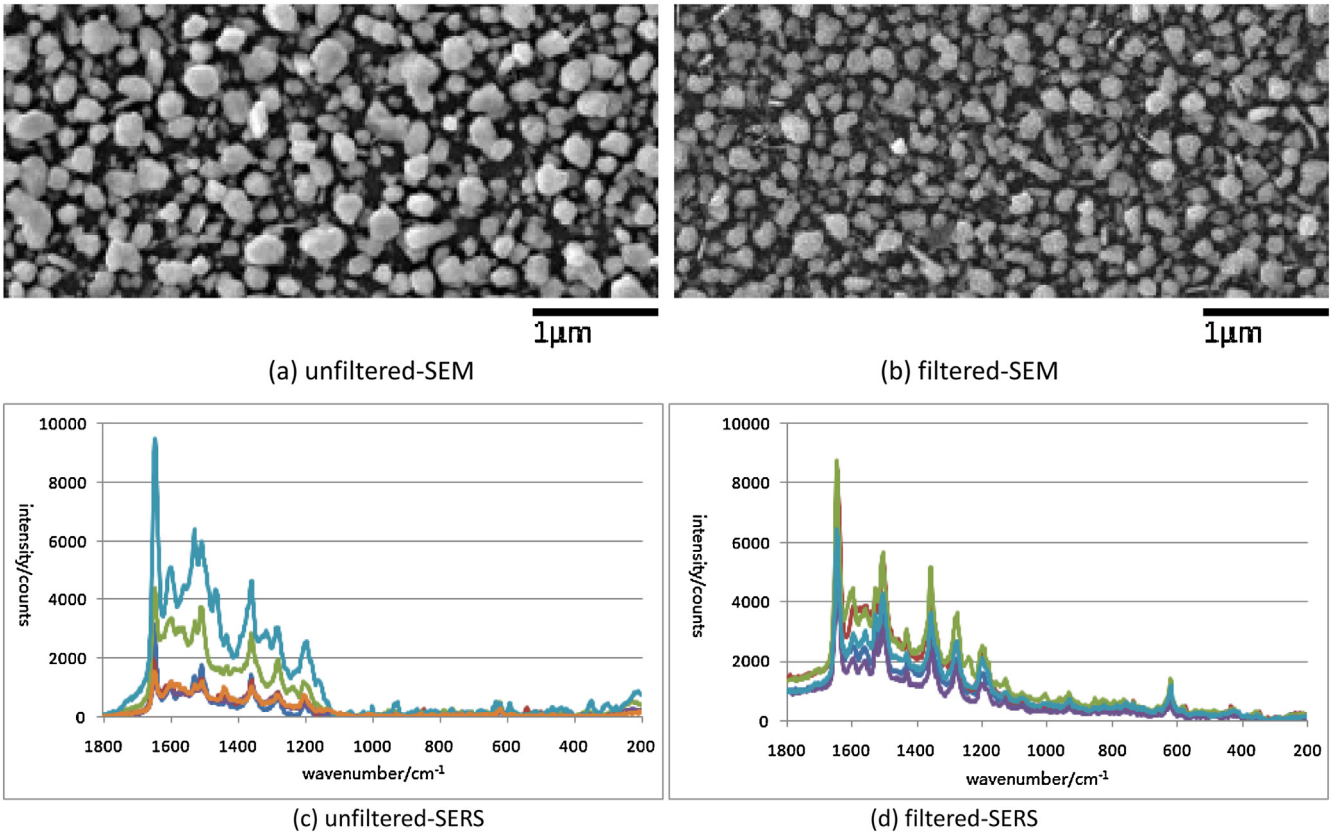

Fig. 5. Comparison between unfiltered and filtered UV catalyzed AgNP substrates.

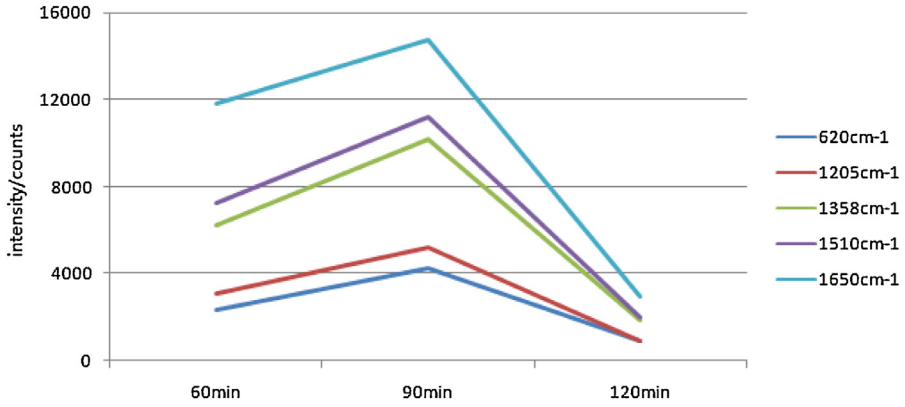

Fig. 6. SERS intensities of the five signature peaks using substrates made with different photo-catalysis times.

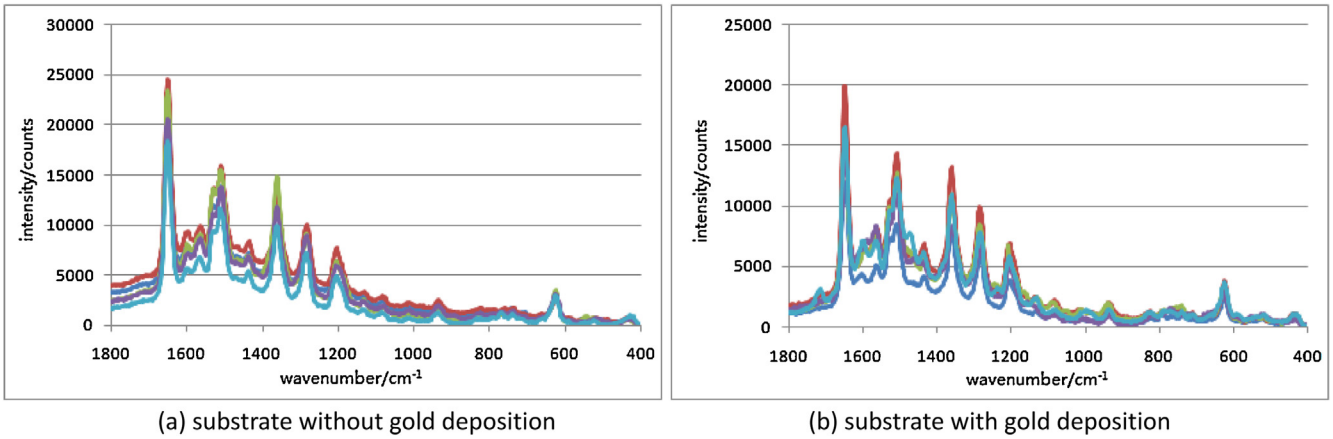

Fig. 7. Comparison between substrate with gold deposition and without gold deposition.

the average intensities for the 1205, 1358, 1510 and 1650 cm^{-1} peaks are 14.3%, 16.9%, 16.8% and 27.9% lower for the substrate with gold deposition. Thus, gold deposition slightly lowers the SERS intensity.

Another experiment is conducted to test the longevity of the substrates. Both substrates are tested again on the 5th, 10th and 15th day to see if SERS signals decayed. 1358 and 1650 cm^{-1} peaks are used for comparison. The results are shown in Table 3. The measurement results from substrate without gold deposition see a fairly sharp decline for both peaks between the 10th day to the 15th day, compared to the substrate with gold deposition. Thus, gold deposition can probably reduce the degradation of the silver SERS substrates. Overall, both types of substrates degrade at a relatively slow rate, consider that the methods proposed in this research can be used to mass produce AgNPs SERS substrates on demand.

4.4. Limit of detection and uniformity

The results of measuring R6G, concentrations from 10^{-6}M to 10^{-8}M are in Fig. 8(a); measurement conditions are as follows: laser is 50 mW 532 nm laser; 5% ND filter is used; measurement time is 3 s. The limit of detection for R6G is 10^{-7}M. However, if measurement time is to 40 s, limit of detection can be lowered to 10^{-8}M, as shown in Fig. 8(b).

Table 3
Substrate longevity experiment for substrates with and without gold deposition.

	Gold depositon				No gold deposition			
	Day 0	Day 5	Day 10	Day 15	Day 0	Day 5	Day 10	Day 15
1350 cm^{-1}	100%	97.6%	94.0%	94.8%	100%	97.8%	93.9%	86.9%
1650 cm^{-1}	100%	92.8%	92.5%	89.5%	100%	93.6%	84.8%	85.5%

The substrates are relative uniform: the following table shows the average values and standard deviation of the 1650 cm^{-1} peak of the ten different measurements on one 5 × 5 mm substrate, for ten substrates. The maximum standard deviation of the 1650 cm^{-1} R6G peak is 16.9% on one substrate. This result indicates good uniformity for SERS measurements. The standard deviation of the averaged values of the ten substrates is 14.5%.

The substrates made using the optimal conditions are used to test a healthy human's blood serum sample as well, as shown in Fig. 9. 785 nm laser is used for serum measurement. Major Raman peaks in Fig. 9 are 637, 724, 821, 853, 886, 957, 1004, 1095, 1130, 1206, 1270, 1320, 1445, 1580 and 1640 cm^{-1}. Peaks are assigned according to recent studies [5]. Most peaks are assigned to uric acid and hypoxanthine; 1270 and 1640 cm^{-1} peaks are assigned to Amide III and Amide I, respectively. The serum spectra clearly show major serum peaks and no abnormal peaks.

5. Conclusion and discussion

This research has found good setups for each step of the process of making TiO_2 photo-catalyzed, silver based SERS enhancement substrate so that the resulting substrates would have good sensitivity and uniformity. The limit of detection for R6G is 10^{-7}M; if the measurement time is increased to 40 s, the limit of detection may be as low as 10^{-8}M. The standard deviation of the R6G signature peak at 1650 cm^{-1} from ten different spots on a

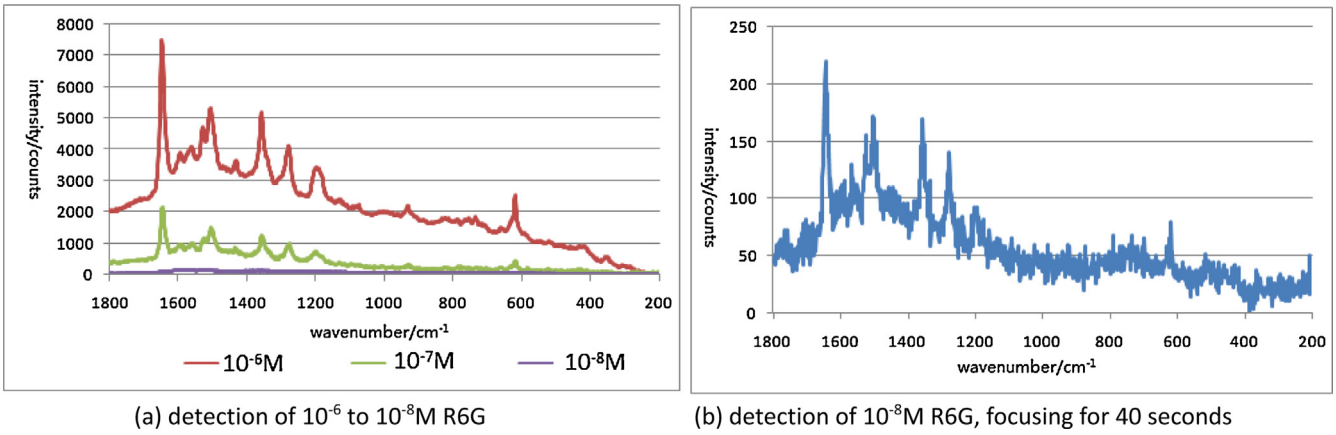

Fig. 8. Limit of detection for Rhodamin 6G using enhancement substrates.

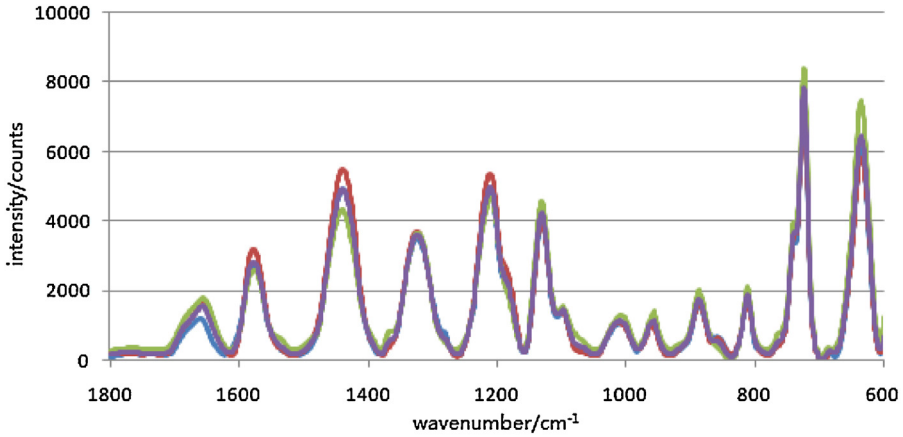

Fig. 9. SERS measurement of human blood serum using the substrates produced in this research.

substrate is 16.9%, less than 20%, which indicates good uniformity for SERS measurements. The standard deviation of the R6G signature peak at 1650 cm^{-1} from ten different substrates is 14.5%, showing that different enhancement substrates have similar performance.

TiO_2 photo-catalysis is not a new way of producing silver nanoparticles; however, it is a cheap, simple and versatile way of producing SERS substrates. Its advantages are that the operations are easy to learn and do not require expensive equipments or reagents; most reagents used in this research except Tetrabutyl titanate and acetylacetonate are common lab reagents. Its disadvantage is that as a self assembly process, it does not allow complete control over the size and distribution of silver nanoparticles. The resulting substrates have decent lifetime; their effectiveness is only reduced by 15% in 15 days, and the lifetime can be further enhanced with gold deposition.

Our research shows that partial control over the size and distribution is possible: different production setups of each step would affect the final distribution of AgNPs on the substrate as well as the final enhancement factor. AgNPs substrates produced using this method have been successfully used in the measurement of human blood serum.

Fundings

National Natural Science Foundation of China (61308067, 61475155); National High Technology Research and Development Program of China (2012AA022602); State Key Laboratory of Applied Optics of China; Administration of Quality Supervision, Inspection and Quarantine of the People's Republic of China (201210094).

References

[1] D.J. Gardiner, Practical Raman Spectroscopy, Springer-Verlag, 1989.
[2] H. Jin, Q. Lu, X. Chen, H. Ding, H. Gao, S. Jin, The use of Raman spectroscopy in food processes: a review, Appl. Spectrosc. Rev. 51 (2015) 12–22.
[3] L.A. Lane, X. Qian, S. Nie, SERS nanoparticles in medicine: from label-free detection to spectroscopic tagging, Chem. Rev. 115 (2015) 10489–10529.
[4] S. Schlucker, Surface-enhanced Raman spectroscopy: concepts and chemical applications, Angew. Chem. 53 (2014) 4756–4795.
[5] A. Bonifacio, S. Cervo, V. Sergo, Label-free surface-enhanced Raman spectroscopy of biofluids: fundamental aspects and diagnostic applications, Anal. Bioanal. Chem. (2015).
[6] M. Fleischmann, P.J. Hendra, A.J. McQuillan, Raman spectra of pyridine adsorbed at a silver electrode, Chem. Phys. Lett. 26 (1974) 163–166.
[7] D.L. Jeanmaire, R.P. Van Duyne, Surface Raman spectroelectrochemistry Part I: heterocyclic, aromatic, and aliphatic amines adsorbed on the anodized silver electrode, J. Electroanal. Chem. 10 (1977) 1–20.
[8] P.L. Stiles, J.A. Dieringer, N.C. Shah, R.P. Van Duyne, Surface-enhanced Raman spectroscopy, Ann. Rev. Anal. Chem. 1 (2008) 601–626.
[9] S. McAughtrie, K. Faulds, D. Graham, Surface enhanced Raman spectroscopy (SERS): potential applications for disease detection and treatment, J. Photochem. Photobiol. C: Photochem. Rev. 21 (2014) 40–53.
[10] Y. Wang, B. Yan, L. Chen, SERS tags: novel optical nanoprobes for bioanalysis, Chem. Rev. 113 (2013) 1391–1428.
[11] X.M. Lin, Y. Cui, Y.H. Xu, B. Ren, Z.Q. Tian, Surface-enhanced Raman spectroscopy: substrate-related issues, Anal. Bioanal. Chem. 394 (2009) 1729–1745.
[12] D. Li, L. Pan, S. Li, K. Liu, S. Wu, W. Peng, Controlled preparation of uniform TiO2-Catalyzed silver nanoparticle films for surface-enhanced Raman scattering, J. Phys. Chem. C 117 (2013) 6861–6871.

[13] Y. Huang, X. Zhang, E. Ringe, M. Hou, L. Ma, Z. Zhang, Tunable lattice coupling of multipole plasmon modes and near-field enhancement in closely spaced gold nanorod arrays, Sci. Rep. 6 (2016) 23159.
[14] P.C. Lee, D. Meisal, Adsorption and surface-enhanced raman of dyes on silver and gold sols, J. Phys. Chem. 86 (1982) 3391–3395.
[15] J. Turkevich, P.C. Stevenson, J. Hillier, The formation of colloid gold, J. Phys. Chem. 57 (1953) 670–673.
[16] A. Tao, F. Kim, H. Hess, J. Goldberger, R. He, Y. Sun, Y. Xia, P. Yang, Langmuir–Blodgett silver nanowire monolayers for molecular sensing using surface-enhanced raman spectroscopy, Nano Lett. 3 (2003) 1229–1233.
[17] B. Nikoobakht, Z.L. Wang, M.A. El-Sayed, Self-assembly of gold nanorods, J. Phys. Chem. B 104 (2000) 8635–8640.
[18] R.G. Freeman, K.C. Grabar, K.J. Allison, R.M. Bright, J.A. Davis, A.P. Guthrie, M.B. Hommer, M.A. Jackson, P.C. Smith, D.G. Walter, M.J. Natan, Self-assembled metal colloid monolayers: an approach to SERS substrates, Science 267 (1995) 1629–1632.
[19] Q. Zhou, Y. He, J. Abell, Z. Zhang, Y. Zhao, Surface-enhanced Raman scattering from helical silver nanorod arrays, Chem. Commun. 47 (2011) 4466–4468.
[20] J.C. Hulteen, D.A. Treichel, M.T. Smith, M.L. Duval, T.R. Jensen, R.P. Van Duyne, Nanosphere lithography: size-tunable silver nanoparticle and surface cluster arrays, J. Phys. Chem. B 103 (1999) 3854–3863.
[21] C.L. Haynes, A.D. McFarland, M.T. Smith, J.C. Hulteen, R.P. Van Duyne, Angle-Resolved nanosphere lithography: manipulation of nanoparticle size, shape, and interparticle spacing, J. Phys. Chem. B 106 (2002) 1898–1902.
[22] A. Mazzocut, E. Coutino-Gonzalez, W. Baekelant, B. Sels, J. Hofkens, T. Vosch, Fabrication of silver nanoparticles with limited size distribution on TiO2 containing zeolites, Phys. Chem. Chem. Phys. 16 (2014) 18690–18693.
[23] P.D. Cozzoli, R. Comparelli, E. Fanizza, M.L. Curri, A. Agostiano, D. Laub, Photocatalytic synthesis of silver nanoparticles stabilized by TiO2 nanorods: a semiconductor/metal nanocomposite in homogeneous nonpolar solution, J. Am. Chem. Soc. 126 (2004) 3868–3879.
[24] X. Liu, Z. Liu, S. Hao, W. Chu, Facile fabrication of well-dispersed silver nanoparticles loading on TiO2 nanotube arrays by electrodeposition, Mater. Lett. 80 (2012) 66–68.
[25] C.Y. Flores, C. Diaz, A. Rubert, G.A. Benitez, M.S. Moreno, M.A. Fernandez Lorenzo de Mele, R.C. Salvarezza, P.L. Schilardi, C. Vericat, Spontaneous adsorption of silver nanoparticles on Ti/TiO2 surfaces. Antibacterial effect on Pseudomonas aeruginosa, J. Colloid Interface Sci. 350 (2010) 402–408.
[26] Q. Zhou, Z. Li, Y. Yang, Z. Zhang, Arrays of aligned, single crystalline silver nanorods for trace amount detection, J. Phys. D: Appl. Phys. 41 (2008) 152007.
[27] P.I. Gouma, M.J. Mills, Anatase-to-rutile transformation in titania powders, J. Am. Ceram. Soc. 84 (2001) 619–622.
[28] L. Ma, Y. Huang, M. Hou, Z. Xie, Z. Zhang, Silver nanorods wrapped with ultrathin Al2O3 layers exhibiting excellent SERS sensitivity and outstanding SERS stability, Sci. Rep. 5 (2015) 12890.